Formation of speckle interference patterns characterizing transversal or longitudinal displacements of a diffusely scattering surface. Part 1

V.G. Gusev

Tomsk State University

Received October 15, 2006

The sensitivity of a speckle interferometer to transversal or longitudinal displacements of a diffusely scattering plane surface is analyzed in the case that a negative lens is used to record a double-exposure specklogram. It is shown that the interferometer sensitivity to transversal displacements depends on the curvature radius of a spherical wave of coherent radiation illuminating the surface. The interferometer sensitivity to longitudinal displacements depends on the scale of the Fourier transform of the function characterizing the complex amplitude of reflection or transmission of the scatterer. Experimental results are in agreement with theoretical arguments.

In the double-exposure recording of quasi-Fourier and Fourier holograms with the use of a negative lens in order to control transversal displacements of a diffusely scattering surface,[1] it was shown that the mechanism of formation of interference patterns in diffracting fields is caused by both tilts and homogeneous displacement of subjective speckles corresponding to the second exposure in the hologram plane relative to identical speckles of the first exposure. At the stage of hologram reconstruction, this circumstance leads to localization of interference patterns in two planes and, for metrological provision, to the necessity to perform the spatial filtering of the diffraction field.

If the longitudinal displacement of a scatterer is controlled, then in the hologram plane we observe, on the one hand, the inhomogeneous displacement of subjective speckles corresponding to the second exposure relative to identical speckles of the first exposure due to the difference in the scales of Fourier transforms of complex transmission (or reflection) amplitudes of a diffusely scattering plane surface in the hologram plane. On the other hand, the tilts of subjective second-exposure speckles relative to identical first-exposure speckles, varying along the radius from the optical axis, cause the localization of interference patterns in two planes. This calls for the necessity of the diffraction field spatial filtering at the stage of hologram reconstruction, for to form the interference pattern by two identical speckles of the both exposures. To do this, it is necessary to reveal features in the correlation of the intensity distribution of light scattered by the surface at the initial and displaced positions of the scatterer, based on distributions of the field complex amplitudes in the plane of the photographic plate.[1]

In this paper, the formation of speckle interference patterns characterizing transversal or longitudinal displacements of a diffusely scattering plane surface is analyzed in order to determine the speckle interferometer sensitivity in the case that a negative lens is used at the stage of the double-exposure recording.

As shown in Fig. 1, a mat screen *1* in the plane (x_1, y_1) is illuminated by coherent radiation with the divergent wave front having the curvature radius R.

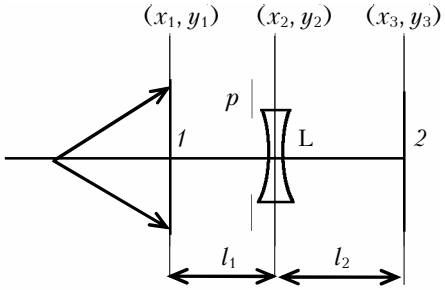

Fig. 1. Diagram of the double-exposure hologram recording: matte screen *1*; photographic plate-specklogram *2*; negative lens L; aperture diaphragm *p*.

The radiation, diffusely scattered by the screen, passes through a thin negative lens L with the focal length f and then is recorded on a photographic plate *2* in the plane (x_3, y_3) for the first exposure time. Before the second exposure, the matte screen is displaced in the plane of its location, for example, in the direction to the axis x by the distance a.

As follows from Ref. 1, the distributions of the field complex amplitudes corresponding to the first and second exposures in the plane of the photographic plate (x_3, y_3) have the form

$$u_1(x_3, y_3) \sim \exp\left[\frac{ik}{2r}\left(x_3^2 + y_3^2\right)\right] \times$$

$$\times\left\{F(x_3, y_3) \otimes \exp\left[-\frac{iklL_0^2}{2l_1^2 l_2^2}\left(x_3^2 + y_3^2\right)\right] \otimes P(x_3, y_3)\right\}, \quad (1)$$

0235-6880/07/08 670-11 $02.00

$$u_2(x_3,y_3)\sim\exp\left[\frac{ik}{2r}\left(x_3^2+y_3^2\right)\right]\exp\left(-\frac{ika^2}{2l}\right)\exp\left(\frac{ikL_0ax_3}{l_1l_2}\right)\times$$
$$\times\left\{F(x_3,y_3)\otimes\exp\left[-\frac{iklL_0^2}{2l_1^2l_2^2}\left(x_3^2+y_3^2\right)\right]\otimes\right.$$
$$\left.\otimes\exp\left(-\frac{ikL_0ax_3}{l_1l_2}\right)P\left(x_3+\frac{l_1l_2}{lL_0}a,y_3\right)\right\},\qquad(2)$$

where $\otimes$ denotes the convolution; k is the wave number; r is the curvature radius of the spherical wave; L_0 is the geometric parameter of the optical system satisfying the condition

$$1/L_0 = 1/l_1 + 1/f + 1/l_2,$$

l_1, l_2 are the distances between the plates (x_1, y_1), (x_2, y_2), and (x_2, y_2), (x_3, y_3); (x_2, y_2) is the main plane of the negative lens L;

$$1/l = 1/R + 1/l_1 - L_0/l_1^2$$

is introduced for brevity; $F(x_3, y_3)$ is the Fourier transform of the complex transmission amplitude $t(x_1, y_1)$ of the matte screen being a random function of coordinates with the spatial frequencies $L_0x_3/\lambda l_1l_2$ and $L_0y_3/\lambda l_1l_2$, λ is the wavelength of the coherent radiation used for the specklogram recording and reconstruction; $P(x_3, y_3)$ is the Fourier transform of the pupil function $p(x_2, y_2)$ [Ref. 2] of the negative lens L with the spatial frequencies $x_3/\lambda l_2$ and $y_3/\lambda l_2$.

If the double-exposure recording of a specklogram is carried out on the linear part of the blackening curve of the photomaterial, then, taking into account that the constant component of transmission occupies a very small spatial area in the plane of recording *3* of the speckle interferogram, its complex transmission amplitude in Fig. 2 is determined as

$$\tau(x_3,y_3)\sim\left\{F(x_3,y_3)\otimes\exp\left[-\frac{iklL_0^2}{2l_1^2l_2^2}\left(x_3^2+y_3^2\right)\right]\otimes P(x_3,y_3)\right\}\times$$
$$\times\{c.c.\}+\left\{F(x_3,y_3)\otimes\exp\left[-\frac{iklL_0^2}{2l_1^2l_2^2}\left(x_3^2+y_3^2\right)\right]\otimes\right.$$
$$\left.\otimes\exp\left(-\frac{ikL_0ax_3}{l_1l_2}\right)P\left(x_3+\frac{l_1l_2}{lL_0}a,y_3\right)\right\}\{c.c.\},\qquad(3)$$

where *c.c.* means complex conjugate.

Let the field diffracting at the specklogram at the stage of hologram recording be bounded by the aperture diaphragm p_0 (see Fig. 2) of a thin positive lens L_0 with the focal length f_0. Then, based on Ref. 3, the distribution of the complex amplitude of the field in the plane (x_5, y_5) takes the form

$$u(x_5,y_5)\sim\int\limits_{-\infty}^{\infty}\int\tau(x_3,y_3)\exp\left[-\frac{ik}{f_0}(x_3x_5+y_3y_5)\right]dx_3dy_3\otimes$$
$$\otimes P_0(x_5,y_5),\qquad(4)$$

where $P_0(x_5, y_5)$ is the Fourier transform of the pupil function $p_0(x_4, y_4)$ [Ref. 2] of the lens L_0 with the spatial frequencies $x_5/\lambda f_0$ and $y_5/\lambda f_0$; (x_4, y_4) is the principal plane of the positive lens.

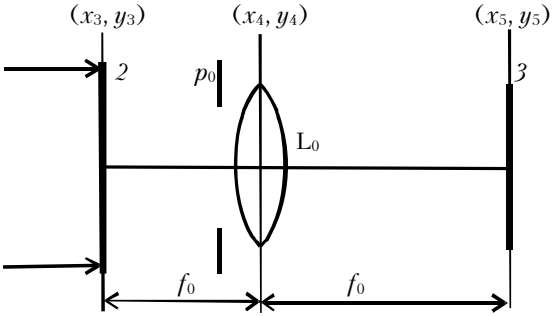

Fig. 2. Diagram of reconstruction of a specklogram characterizing a transversal displacement of the scatterer: specklogram *2*; plane of recording *3* of the speckle interferogram; positive lens L_0; aperture diaphragm p_0.

After the substitution of Eq. (3) into Eq. (4) taking into account the parity of $p(x_2, y_2)$, we obtain

$$u(x_5,y_5)\sim\left\{\left\{p\left(\frac{l_2}{f_0}x_5,\frac{l_2}{f_0}y_5\right)t\left(-\frac{l_1l_2}{L_0f_0}x_5,-\frac{l_1l_2}{L_0f_0}y_5\right)\times\right.\right.$$
$$\times\exp\left[\frac{ikl_1^2l_2^2}{2L_0^2f_0^2}\left(x_5^2+y_5^2\right)\right]\otimes p\left(\frac{l_2}{f_0}x_5,\frac{l_2}{f_0}y_5\right)t^*\left(\frac{l_1l_2}{L_0f_0}x_5,\frac{l_1l_2}{L_0f_0}y_5\right)\times$$
$$\left.\times\exp\left[-\frac{ikl_1^2l_2^2}{2L_0^2f_0^2}\left(x_5^2+y_5^2\right)\right]\right\}+\left\{p\left(\frac{l_2}{f_0}x_5+\frac{L_0}{l_1}a,\frac{l_2}{f_0}y_5\right)\times\right.$$
$$\times t\left(-\frac{l_1l_2}{L_0f_0}x_5,-\frac{l_1l_2}{L_0f_0}y_5\right)\exp\left[\frac{ikl_1^2l_2^2}{2lL_0^2f_0^2}\left(x_5^2+y_5^2\right)\right]\times$$
$$\times\exp\left(\frac{ikl_1l_2ax_5}{lL_0f_0}\right)\otimes p\left(\frac{l_2}{f_0}x_5-\frac{L_0}{l_1}a,\frac{l_2}{f_0}y_5\right)t^*\left(\frac{l_1l_2}{L_0f_0}x_5,\frac{l_1l_2}{L_0f_0}y_5\right)\times$$
$$\left.\left.\times\exp\left[-\frac{ikl_1^2l_2^2}{2lL_0^2f_0^2}\left(x_5^2+y_5^2\right)\right]\exp\left(\frac{ikl_1l_2ax_5}{lL_0f_0}\right)\right\}\right\}\otimes P_0(x_5,y_5).\qquad(5)$$

It follows from Eq. (5) that within the area, determined by the width of the function

$$p(l_2x_5/f_0,l_2y_5/f_0)\otimes p(l_2x_5/f_0,l_2y_5/f_0),$$

the subjective speckle field with the speckle size determined by the $P_0(x_5, y_5)$ width takes place in the plane (x_5, y_5).

Assume that when calculating the illumination distribution

$$I(x_5,y_5) = u(x_5,y_5)u^*(x_5,y_5)$$

in the recording plane *3* (see Fig. 2), in order to exclude the speckle effect from the consideration, the averaging is performed over the area exceeding the domain of existence of a subjective speckle, but within which the phase $kl_1l_2ax_5/lL_0f_0$ does not change. In addition, we believe that, as in the literature,[4,5] the random function is delta-correlated, that is, taking into account the homogeneity of a random parameter

$$\left\langle t\left[-l_1l_2(x_5-\xi)/L_0f_0,-l_1l_2(y_5-\eta)/L_0f_0\right]\times\right.$$
$$\times t^*\left[-l_1l_2(x_5-\xi')/L_0f_0,-l_1l_2(y_5-\eta')/L_0f_0\right]\times$$
$$\left.\times t^*(l_1l_2\xi/L_0f_0,l_1l_2\eta/L_0f_0)t(l_1l_2\xi'/L_0f_0,l_1l_2\eta'/L_0f_0)\right\rangle\sim$$
$$\sim\delta(\xi-\xi')\delta(\eta-\eta'),$$

where the angular brackets denote the averaging; $\delta(\xi-\xi')\delta(\eta-\eta')$ is the Dirac delta function. Then the illumination distribution in the plane (x_5, y_5) takes the form

$$I(x_5,y_5)\sim 1+\upsilon\cos\left(\frac{kl_1l_2ax_5}{lL_0f_0}\right), \qquad (6)$$

where υ is the visibility of the interference pattern. The real function

$$\upsilon = p'(x_5,y_5)\otimes p'(x_5,y_5)/p(x_5,y_5)\otimes p(x_5,y_5),$$

where $p'(x_5,y_5)$ is the function equal to unity within overlapping areas $p(x_5,y_5)$, $p(x_5+L_0f_0a/l_1l_2,y_5)$ and equal to zero beyond this area.

According to Eq. (6), interference fringes are located equidistantly on the axis x in the recording plane *3* (see Fig. 2). Measuring the periods of these fringes, it is possible to determine the transversal displacement of the diffusely scattering plane surface. The period

$$\Delta x_5' = \lambda f_0/(1+l_2/f+l_1l_2/RL_0)a$$

for fixed values of λ, f, f_0, l_1, and l_2 depends on the curvature radius of the divergent spherical wave of the coherent radiation used to illuminate the matte screen *1* (see Fig. 1) at the stage of the double-exposure recording of a specklogram. In addition, the interferometer sensitivity increases with the decrease of R, which is explained by the increase of the homogeneous displacement of subjective second-exposure speckles with respect to identical first-exposure speckles in the specklogram plane. As an example, the dependence of the frequency of interference fringes on the curvature radius is shown in Fig. 3 for $\lambda=0.6328$ μm, $a=25$ μm, $f=220$ mm, $f_0=50$ mm, $l_1=160$ mm, $l_2=160$ mm.

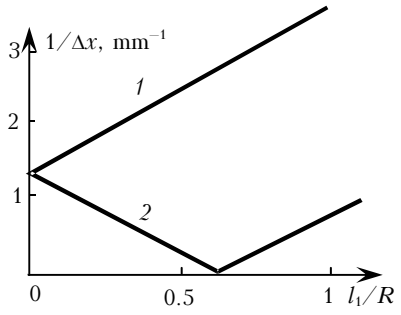

Fig. 3. Frequency of interference fringes for fixed λ, f, f_0, l_1, and l_2 as a function of the curvature radius of a (*1*) divergent and (*2*) convergent spherical wave.

As the sign of the curvature radius of the wave front in the plane (x_1, y_1) (see Fig. 1) alternates, the period of interference fringes

$$\Delta x_5'' = \lambda f_0/(1+l_2/f-l_1l_2/RL_0)a$$

increases, when R decreases in the range $l_1^2/(l_1-L_0)\le R\le\infty$. The condition $R'=l_1^2/(l_1-L_0)$ corresponds to the condition of formation of the field complex amplitude distribution corresponding to the Fourier transform of $t(x_1, y_1)$ [Ref. 6] in Eq. (1) and to the absence of displacements of subjective second-exposure speckles in the specklogram plane. Further decrease of R leads to the increase in the interferometer sensitivity due to the appearance and growth of the homogeneous displacement of subjective second-exposure speckles in the specklogram plane.

Assume that at the stage of reconstruction of a double-exposure specklogram, characterizing the transversal displacement of the diffusely scattering plane surface, the specklogram displaces in the plane (x_3, y_3) (see Fig. 2) by x_{03}. Then the complex transmission amplitude of the specklogram is determined as

$$\tau(x_3,y_3)\sim\left\{F(x_3+x_{03},y_3)\otimes\right.$$
$$\otimes\exp\left\{-\frac{iklL_0^2}{2l_1^2l_2^2}\left[(x_3+x_{03})^2+y_3^2\right]\right\}\otimes P(x_3,y_3)\Bigg\}\{c.c.\}+$$
$$+\left\{F(x_3+x_{03},y_3)\otimes\exp\left\{-\frac{iklL_0^2}{2l_1^2l_2^2}\left[(x_3+x_{03})^2+y_3^2\right]\right\}\otimes\right.$$
$$\left.\otimes\exp\left[-\frac{ikL_0a}{l_1l_2}(x_3+x_{03})\right]P\left(x_3+\frac{l_1l_2}{lL_0}a,y_3\right)\right\}\{c.c.\}, \qquad (7)$$

and the distribution of the field complex amplitude in the plane (x_5, y_5) takes the form

$$u(x_5,y_5)\sim\left\{\left\{p\left(\frac{l_2}{f_0}x_5,\frac{l_2}{f_0}y_5\right)t\left(-\frac{l_1l_2}{L_0f_0}x_5,-\frac{l_1l_2}{L_0f_0}y_5\right)\times\right.\right.$$
$$\times\exp\left[\frac{ikl_1^2l_2^2}{2lL_0^2f_0^2}\left(x_5^2+y_5^2\right)\right]\exp(i2kx_{03}x_5/f_0)\otimes$$
$$\otimes p\left(\frac{l_2}{f_0}x_5,\frac{l_2}{f_0}y_5\right)t^*\left(\frac{l_1l_2}{L_0f_0}x_5,\frac{l_1l_2}{L_0f_0}y_5\right)\times$$
$$\left.\times\exp\left[-\frac{ikl_1^2l_2^2}{2lL_0^2f_0^2}\left(x_5^2+y_5^2\right)\right]\exp(i2kx_{03}x_5/f_0)\right\}+$$
$$+\left\{p\left(\frac{l_2}{f_0}x_5+\frac{L_0a}{l_1},\frac{l_2}{f_0}y_5\right)t\left(-\frac{l_1l_2}{L_0f_0}x_5,-\frac{l_1l_2}{L_0f_0}y_5\right)\times\right.$$
$$\times\exp\left[\frac{ikl_1^2l_2^2}{2lL_0^2f_0^2}\left(x_5^2+y_5^2\right)\right]\exp(i2kx_{03}x_5/f_0)\times$$
$$\times\exp(ikl_1l_2ax_5/lL_0f_0)\otimes p\left(\frac{l_2}{f_0}x_5-\frac{L_0}{l_1}a,\frac{l_2}{f_0}y_5\right)\times$$
$$\left.\left.\times t^*\left(\frac{l_1l_2}{L_0f_0}x_5,\frac{l_1l_2}{L_0f_0}y_5\right)\exp\left[-\frac{ikl_1^2l_2^2}{2lL_0^2f_0^2}\left(x_5^2+y_5^2\right)\right]\times\right.\right.$$
$$\left.\left.\times\exp(i2kx_{03}/f_0)\exp(ikl_1l_2ax_5/lL_0f_0)\right\}\right\}\otimes P_0(x_5,y_5). \qquad (8)$$

The above calculations for determination of the illumination distribution in the plane (x_5, y_5) yield the equation corresponding to Eq. (6). Consequently, in case of the speckle interference control over the transversal displacement of a diffusely scattering plane surface, "frozen" interference fringes are observed, and there is no need in the spatial filtering of the diffraction field for their recording.

The comparison of the holographic interferometer,[1] which records the interference pattern located in the Fourier plane, and the speckle interferometer under consideration shows that their sensitivity to the transversal displacement of a scatterer is identical. This is explained by the fact that the nature of the mechanism of formation of interference patterns consists in the homogeneous displacement of subjective second-exposure speckles in the hologram or specklogram plane. In the speckle interferometer regardless of the curvature radius of the spherical wave front in the plane (x_1, y_1) (see Fig. 1), the visibility of interference fringes is lower than unity. This is because in the holographic interferometer two images of the negative lens pupil are formed in the Fourier plane, and the interference pattern is formed within these two images overlapping. In the speckle interferometer, the image of the negative lens pupil is not formed in the Fourier plane, and the visibility of interference fringes is lower than unity due to the background radiation caused by the diffraction from nonoverlapping areas. However, for small transversal displacements of the scatterer, when $L_0 f_0 a / l_1 l_2$ is much smaller than the pupil radius of the negative lens, the difference from unity is small. In addition, in the speckle interferometer as compared to the holographic interferometer,[1] the threshold sensitivity to the transversal displacement of a diffusely scattering plane surface decreases due to the increase in the spatial length of the interference pattern in speckle interferometry.[7]

It should be noted that the indirect studies (see, for example, Refs. 8 and 9) connected with formation of lateral-shear holographic interferograms with a negative lens used at the stage of recording, are accompanied by the formation of speckle interference patterns in the zero diffraction order. These patterns are formed, if the above dependence of the subjective second-exposure speckles displacement with respect to identical first-exposure speckles in the plane of the recording medium on the curvature radius of the wave front of the coherent radiation, used for illumination of a scatterer, is taken into account.

Let the matte screen before the second exposure of the photographic plate *2* (see Fig. 1), is shifted along the axis z by the distance $\Delta l \ll l_1$. Then, based on Ref. 1, the distribution of the field complex amplitude, corresponding to the second exposure in the plane of the photographic plate, is determined as

$$u_2'(x_3, y_3) \sim \exp(ik\Delta l)\exp\left[\frac{ik}{2r}\left(x_3^2 + y_3^2\right)\right] \times$$
$$\times \exp\left[-\frac{ikL_0^2\Delta l}{2l_1^2 l_2^2}\left(x_3^2 + y_3^2\right)\right]\left\{F'(x_3, y_3) \otimes\right.$$
$$\left.\otimes \exp\left[-\frac{ikl'L_0^2}{2\left(l_1 + \Delta l\right)^2 l_2^2}\left(x_3^2 + y_3^2\right)\right] \otimes P(x_3, y_3)\right\}, \qquad (9)$$

where $F'(x_3, y_3)$ is the Fourier transform of $t(x_1, y_1)$ with the spatial frequencies

$$L_0' x_3/\lambda\left(l_1+\Delta l\right)l_2,\ L_0' y_3/\lambda\left(l_1+\Delta l\right)l_2;\ L_0' = L_0\left(1+L_0\Delta l/l_1^2\right);$$
$$1/l' = 1/\left(l_1 + \Delta l\right) + 1/\left(R - \Delta l\right) - L_0'/\left(l_1 + \Delta l\right)^2.$$

According to Eq. (9), subjective second-exposure speckles are shifted along the radius from the optical axis relative to identical first-exposure speckles due to the difference in the scales of Fourier transforms $F(x_3, y_3)$, $F'(x_3, y_3)$ in Eqs. (1) and (9). This inhomogeneous speckle shift is independent of the spherical wave curvature radius of the coherent radiation used to illuminate the scatterer. The tilt of subjective speckles, varying along the radius from the optical axis and determined by the presence of the factor $\exp[-ikL_0^2\Delta l(x_3^2+y_3^2)/2l_1^2l_2^2]$ in Eq. 9, is independent of the curvature radius as well. In its turn, due to the orientation character of subjective second-exposure speckles, there exists an additional variation of the tilt along the radius from the optical axis, which depends on the curvature radius of the wave front in the plane (x_1, y_1) (see Fig. 1) and is determined by the factor under the integral of function convolutions in Eq. (9). In the general case, this circumstance leads to a significant decorrelation of the speckle structures of the both exposures. The decorrelation is absent, if the scatterer is illuminated by the coherent radiation with the divergent or convergent spherical wave with the curvature radius $R' = l_1^2/(l_1 - L_0)$ [Ref. 1]. Therefore, to prove the possibility of formation of a high-contrast speckle interference pattern characterizing the longitudinal displacement of a diffusely scattering plane surface, we restrict our consideration to this value of R' of the wave front. Then, neglecting the constant component of transmission, the distribution of the complex transmission amplitude $\tau'(x_3, y_3)$ of the double-exposure specklogram (Fig. 4) takes the form

$$\tau'(x_3, y_3) \sim \left\{F(x_3, y_3) \otimes \exp\left[-\frac{ikR'L_0^2}{4l_1^2 l_2^2}\left(x_3^2 + y_3^2\right)\right] \otimes\right.$$
$$\left.\otimes P(x_3, y_3)\right\}\{k.c.\} + \left\{F'(x_3, y_3) \otimes\right.$$
$$\left.\otimes \exp\left[-\frac{ikR'L_0^2}{4l_1^2 l_2^2}\left(x_3^2 + y_3^2\right)\right] \otimes P(x_3, y_3)\right\}\{c.c.\}, \qquad (10)$$

where spatial frequencies of the Fourier transform $F'(x_3, y_3)$ correspond to

$$L_0 x_3/\lambda l_1 l_2(1+\Delta l/R'),\ \ L_0 y_3/\lambda l_1 l_2(1+\Delta l/R').$$

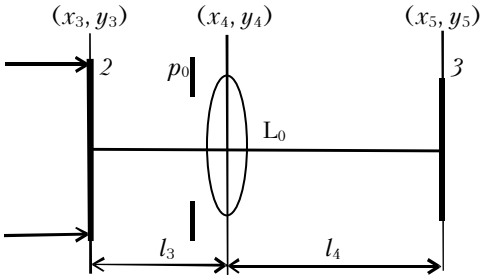

Fig. 4. Diagram of reconstruction of a specklogram characterizing the longitudinal displacement of a scatterer: specklogram *2*; plane of recording *3* of speckle interferograms; positive lens L_0; aperture diaphragm p_0.

Assume that at the stage of specklogram reconstruction the specklogram-scattered radiation is recorded in the plane (x_5, y_5) with the use of a thin positive lens L_0 with the focal length f_0. Then the distribution of the complex amplitude in this plane in the Fresnel approximation is determined as

$$u'(x_5,y_5)\sim\iiiint_{-\infty}^{\infty}\tau'(x_3,y_3)\exp\left\{\frac{ik}{2l_3}\left[(x_3-x_4)^2+(y_3-y_4)^2\right]\right\}\times$$
$$\times p_0(x_4,y_4)\exp\left[-\frac{ik}{2f_0}\left(x_4^2+y_4^2\right)\right]\times$$
$$\times\exp\left\{\frac{ik}{2l_4}\left[(x_4-x_5)^2+(y_4-y_5)^2\right]\right\}\mathrm{d}x_3\mathrm{d}y_3\,\mathrm{d}x_4\mathrm{d}y_4, \quad (11)$$

where (x_4, y_4) is the principal plane of the lens L_0; l_3, l_4 are respectively the distances between the planes (x_3, y_3), (x_4, y_4) and (x_4, y_4), (x_5, y_5).

After transformations well-known in the Fourier optics, we obtain

$$u'(x_5,y_5)\sim\exp\left[\frac{ik}{2l_4}\left(x_5^2+y_5^2\right)\right]\times$$
$$\times\left\{\tau'\left(-\frac{l_3}{l_4}x_5,-\frac{l_3}{l_4}y_5\right)\exp\left[\frac{ikl_3}{2l_4^2}\left(x_5^2+y_5^2\right)\right]\otimes\right.$$
$$\left.\otimes\exp\left[-\frac{ik\mu l_3}{2\tilde{l}l_4}\left(x_5^2+y_5^2\right)\right]\otimes P_0'(x_5,y_5)\right\}, \quad (12)$$

where $\mu=\left(\tilde{l}+l_3\right)/l_4$ is the coefficient of scale transformation, which follows from the condition

$$1/f_0=1/\left(\tilde{l}+l_3\right)+1/l_4;P_0'(x_5,y_5),$$

being the Fourier transform of the pupil function $p_0(x_4, y_4)$ of the lens L_0 with the spatial frequencies $x_5/\lambda l_4, y_5/\lambda l_4$.

According to Eq. (12), the subjective speckle field is formed in the recording plane *3* (see Fig. 4). This field is characterized by the speckle size determined by the width of $P_0'(x_5, y_5)$, and the phase distribution of the divergent spherical wave with the curvature radius l_4 is superimposed on this field.

After substitution of Eq. (10) in Eq. (12), the distribution of the field complex amplitude in the plane (x_5, y_5) takes the form

$$u'(x_5,y_5)\sim\exp\left[\frac{ik}{2l_4}\left(x_5^2+y_5^2\right)\right]\left\{\exp\left[\frac{ikl_3}{2l_4^2}\left(x_5^2+y_5^2\right)\right]\times\right.$$
$$\times\left\{\left\{F\left(-\frac{l_3}{l_4}x_5,-\frac{l_3}{l_4}y_5\right)\otimes\exp\left[-\frac{ikR'L_0^2l_3^2}{4l_1^2l_2^2l_4^2}\left(x_5^2+y_5^2\right)\right]\otimes\right.\right.$$
$$\left.\left.\otimes P\left(-\frac{l_3}{l_4}x_5,-\frac{l_3}{l_4}y_5\right)\right\}\{k.c.\}+\left\{F'\left(-\frac{l_3}{l_4}x_5,-\frac{l_3}{l_4}y_5\right)\otimes\right.\right.$$
$$\left.\left.\otimes\exp\left[-\frac{ikR'L_0^2l_3^2}{4l_1^2l_2^2l_4^2}\left(x_5^2+y_5^2\right)\right]\otimes P\left(-\frac{l_3}{l_4}x_5,-\frac{l_3}{l_4}y_5\right)\right\}\{c.c.\}\right\}\otimes$$
$$\left.\otimes\exp\left[-\frac{ik\mu l_3}{2\tilde{l}l_4}\left(x_5^2+y_5^2\right)\right]\otimes P_0'(x_5,y_5)\right\}. \quad (13)$$

As a result of the integral representation of the convolution operation with the function

$$\exp[-ik\mu l_3(x_5^2+y_5^2)/2\tilde{l}l_4]$$

in Eq. (13), we obtain

$$u'(x_5,y_5)\sim\exp\left[\frac{ik}{2l_4}\left(x_5^2+y_5^2\right)\right]\left\{\exp\left[-\frac{ik\mu l_3}{2\tilde{l}l_4}\left(x_5^2+y_5^2\right)\right]\times\right.$$
$$\times\left\{\exp\left[\frac{ik\mu^2}{2\tilde{l}}\left(x_5^2+y_5^2\right)\right]\otimes\left\{p\left(\frac{l_2\mu}{\tilde{l}}x_5,\frac{l_2\mu}{\tilde{l}}y_5\right)\times\right.\right.$$
$$\times t\left(-\frac{l_1l_2\mu}{\tilde{l}L_0}x_5,-\frac{l_1l_2\mu}{\tilde{l}L_0}y_5\right)\exp\left[\frac{ikl_1^2l_2^2\mu^2}{\tilde{l}^2R'L_0^2}\left(x_5^2+y_5^2\right)\right]\otimes$$
$$\otimes p\left(\frac{l_2\mu}{\tilde{l}}x_5,\frac{l_2\mu}{\tilde{l}}y_5\right)t^*\left(\frac{l_1l_2\mu}{\tilde{l}L_0}x_5,\frac{l_1l_2\mu}{\tilde{l}L_0}y_5\right)\times$$
$$\times\exp\left[-\frac{ikl_1^2l_2^2\mu^2}{\tilde{l}^2R'L_0^2}\left(x_5^2+y_5^2\right)\right]+p\left(\frac{l_2\mu}{\tilde{l}}x_5,\frac{l_2\mu}{\tilde{l}}y_5\right)\times$$
$$\times t\left[-\frac{l_1l_2}{\tilde{l}L_0}\mu\left(1+\frac{\Delta l}{R'}\right)x_5,-\frac{l_1l_2}{\tilde{l}L_0}\mu\left(1+\frac{\Delta l}{R'}\right)y_5\right]\times$$
$$\times\exp\left[\frac{ikl_1^2l_2^2\mu^2}{\tilde{l}^2R'L_0^2}\left(x_5^2+y_5^2\right)\right]\otimes p\left(\frac{l_2}{\tilde{l}}\mu x_5,\frac{l_2}{\tilde{l}}\mu y_5\right)\times$$
$$\times t^*\left[\frac{l_1l_2}{\tilde{l}L_0}\mu\left(1+\frac{\Delta l}{R'}\right)x_5,\frac{l_1l_2}{\tilde{l}L_0}\mu\left(1+\frac{\Delta l}{R'}\right)y_5\right]\times$$
$$\left.\left.\left.\times\exp\left[-\frac{ikl_1^2l_2^2\mu^2}{\tilde{l}^2R'L_0^2}\left(x_5^2+y_5^2\right)\right]\right]\right\}\otimes P_0'(x_5,y_5)\right\}. \quad (14)$$

For $\Delta l << R'$

$$t\left[-l_1 l_2 \mu(1+\Delta l/R')x_5/\tilde{l}L_0, -l_1 l_2 \mu(1+\Delta l/R')y_5/\tilde{l}L_0\right] =$$

$$= t\left(-l_1 l_2 \mu x_5/\tilde{l}L_0, -l_1 l_2 \mu y_5/\tilde{l}L_0\right) \otimes \exp\left[\frac{-ikl_1^2 l_2^2 \mu^2 \left(x_5^2+y_5^2\right)}{2\tilde{l}^2 L_0^2 \Delta l}\right],$$

and taking into account that $\tau'(x_3, y_3)$ is a real function:

$$t^*\left[l_1 l_2 \mu(1+\Delta l/R')x_5/\tilde{l}L_0, l_1 l_2 \mu(1+\Delta l/R')y_5/\tilde{l}L_0\right] =$$

$$= t^*\left(l_1 l_2 \mu x_5/\tilde{l}L_0, l_1 l_2 \mu y_5/\tilde{l}L_0\right) \otimes \exp\left[\frac{-ikl_1^2 l_2^2 \mu^2 \left(x_5^2+y_5^2\right)}{2\tilde{l}^2 L_0^2 \Delta l}\right].$$

Then, as a result of the integral representation of the convolution with the function

$$\exp[ik\mu^2(x_5^2+y_5^2)/2\tilde{l}]$$

in Eq. (14), the distribution of the complex amplitude of the field in the plane (x_5, y_5) takes the form

$$u'(x_5,y_5) \sim \exp\left[\frac{ik}{2l_4}\left(x_5^2+y_5^2\right)\right]\left\{\exp\left[-\frac{ik\mu l_3}{2\tilde{l}l_4}\left(x_5^2+y_5^2\right)\right]\times\right.$$

$$\times\exp\left[\frac{ik\mu^2}{2\tilde{l}}\left(x_5^2+y_5^2\right)\right]\left\{\exp\left[-\frac{ik\mu^2}{2\tilde{l}}\left(x_5^2+y_5^2\right)\right]\otimes\right.$$

$$\otimes\left\{\left\{F_1(x_5,y_5)\otimes\exp\left[-\frac{ikR'L_0^2\mu^2}{4l_1^2l_2^2}\left(x_5^2+y_5^2\right)\right]\otimes P'(x_5,y_5)\right\}\times\right.$$

$$\times\left\{F_2(x_5,y_5)\otimes\exp\left[\frac{ikR'L_0^2\mu^2}{4l_1^2l_2^2}\left(x_5^2+y_5^2\right)\right]\otimes P'(x_5,y_5)\right\}+$$

$$+\left\{\exp\left[\frac{ikL_0^2\mu^2\Delta l}{2l_1^2l_2^2}\left(x_5^2+y_5^2\right)\right]F_1(x_5,y_5)\otimes\right.$$

$$\otimes\exp\left[-\frac{ikR'L_0^2\mu^2}{4l_1^2l_2^2}\left(x_5^2+y_5^2\right)\right]\otimes P'(x_5,y_5)\Bigg\}\times$$

$$\times\left\{\exp\left[\frac{ikL_0^2\mu^2\Delta l}{2l_1^2l_2^2}\left(x_5^2+y_5^2\right)\right]F_2(x_5,y_5)\otimes\right.$$

$$\left.\left.\left.\left.\otimes\exp\left[\frac{ikR'L_0^2\mu^2}{4l_1^2l_2^2}\left(x_5^2+y_5^2\right)\right]\otimes P'(x_5,y_5)\right\}\right\}\right\}P_0'(x_5,y_5)\Bigg\}, \quad (15)$$

where $F_1(x_5,y_5)$, $F_2(x_5,y_5)$ are respectively the Fourier transforms of the functions

$$t\left(-l_1 l_2 \mu\xi/\tilde{l}L_0, -l_1 l_2 \mu\eta/\tilde{l}L_0\right), \quad t^*\left(l_1 l_2 \mu\xi/\tilde{l}L_0, l_1 l_2 \mu\eta/\tilde{l}L_0\right)$$

with the spatial frequencies $\mu^2 x_5/\lambda\tilde{l}, \mu^2 y_5/\lambda\tilde{l}$; $P'(x_5, y_5)$ is the Fourier transform of $p(l_2\mu\xi/\tilde{l}, l_2\mu\eta/\tilde{l})$ with the spatial frequencies $\mu^2 x_5/\lambda\tilde{l}, \mu^2 y_5/\lambda\tilde{l}$.

Since

$$kL_0^2\mu^2\Delta l(x_5^2+y_5^2)/l_1^2l_2^2 << k\mu^2(x_5^2+y_5^2)/2\tilde{l},$$

the function $\exp[ikL_0^2\mu^2\Delta l(x_5^2+y_5^2)/l_1^2l_2^2]$ can be factored out of the integrals of convolution with the functions

$$\exp\left[ikR'L_0^2\mu^2\left(x_5^2+y_5^2\right)/4l_1^2l_2^2\right],\ P'(x_5,\ y_5),$$

$$\exp[-ik\mu^2(x_5^2+y_5^2)/2\tilde{l}].$$

into Eq. (15) because it varies slowly with the coordinate. In addition, we assume that the subjective speckle size in the recording plane *3* (see Fig. 4) is at least an order of magnitude[10] smaller than the period of variation of $1+\exp[ikL_0^2\mu^2\Delta l(x_5^2+y_5^2)/l_1^2l_2^2]$. Then, taking into account the integral representation of the convolution operation in Eq. (15), the illumination distribution in the plane (x_5, y_5) is determined by the equation

$$I'(x_5,y_5) \sim \left\{1+\cos\left[\frac{kL_0^2\mu^2\Delta l}{l_1^2l_2^2}\left(x_5^2+y_5^2\right)\right]\right\}\times$$

$$\times\left|\exp\left[-\frac{ik\mu l_3}{2\tilde{l}l_4}\left(x_5^2+y_5^2\right)\right]\left\{\exp\left[\frac{ik\mu^2}{2\tilde{l}}\left(x_5^2+y_5^2\right)\right]\otimes\right.\right.$$

$$\otimes p\left(\frac{l_2\mu}{\tilde{l}}x_5, \frac{l_2\mu}{\tilde{l}}y_5\right)t\left(-\frac{l_1l_2}{\tilde{l}L_0}\mu x_5, -\frac{l_1l_2}{\tilde{l}L_0}\mu y_5\right)\times$$

$$\times\exp\left[\frac{ikl_1^2l_2^2\mu^2}{\tilde{l}^2R'L_0^2}\left(x_5^2+y_5^2\right)\right]\otimes p\left(\frac{l_2\mu}{\tilde{l}}x_5, \frac{l_2\mu}{\tilde{l}}y_5\right)\times$$

$$\left.\left.\times t^*\left(\frac{l_1l_2}{\tilde{l}L_0}\mu x_5, \frac{l_1l_2}{\tilde{l}L_0}\mu y_5\right)\exp\left[-\frac{ikl_1^2l_2^2\mu^2}{\tilde{l}^2R'L_0^2}\left(x_5^2+y_5^2\right)\right]\right\}\otimes\right.$$

$$\left.\otimes P_0'(x_5,y_5)\right|^2. \quad (16)$$

If at the stage of the double-exposure recording of a specklogram the matte screen *1* (see Fig. 1) is illuminated by the coherent radiation with the convergent spherical wave of the curvature radius $R' = l_1^2/(l_1 - L_0)$, then the illumination distribution in the plane (x_5, y_5) is similar to Eq. (16), that is,

$$I'(x_5,y_5) \sim \left\{1+\cos\left[\frac{kL_0^2\mu^2\Delta l}{l_1^2l_2^2}\left(x_5^2+y_5^2\right)\right]\right\}\times$$

$$\times\left|\exp\left[-\frac{ik\mu l_3}{2\tilde{l}l_4}\left(x_5^2+y_5^2\right)\right]\times\left\{\exp\left[\frac{ik\mu^2}{2\tilde{l}}\left(x_5^2+y_5^2\right)\right]\otimes\right.\right.$$

$$\otimes p\left(\frac{l_2\mu}{\tilde{l}}x_5, \frac{l_2\mu}{\tilde{l}}y_5\right)t\left(-\frac{l_1l_2}{\tilde{l}L_0}\mu x_5, -\frac{l_1l_2}{\tilde{l}L_0}\mu y_5\right)\otimes$$

$$\left.\left.\otimes p\left(\frac{l_2\mu}{\tilde{l}}x_5, \frac{l_2\mu}{\tilde{l}}y_5\right)\times t^*\left(\frac{l_1l_2}{\tilde{l}L_0}\mu x_5, \frac{l_1l_2}{\tilde{l}L_0}\mu y_5\right)\right\}\otimes P_0'(x_5,y_5)\right|^2, \quad (17)$$

which differs only by the different illumination distribution in the subjective speckle structure.

It follows from Eqs. (16) and (17) that in the plane (x_5, y_5) within the area determined by the width of the function

$$p\left(l_2\mu x_5/\tilde{l}, l_2\mu y_5/\tilde{l}\right) \otimes p\left(l_2\mu x_5/\tilde{l}, l_2\mu y_5/\tilde{l}\right),$$

the subjective speckle structure is modulated by fringes of equal tilt, namely, the system of concentric interference fringes, the measurement of whose radii in neighboring interference orders ensures the possibility of determining the longitudinal displacement of a diffusely scattering plane surface for the known values of λ, μ, L_0, l_1, and l_2. In addition, the speckle interferometer sensitivity to the longitudinal displacement of a scatterer depends on L_0/l_1l_2, which determines (in the specklogram plane) the scale of the Fourier transform of the function characterizing the complex transmission amplitude of the matte screen *1* (see Fig. 1) in the plane (x_1, y_1). The sensitivity increases with the scale decrease of the Fourier transform $F(x_3, y_3)$, because this circumstance leads to the increase of the inhomogeneous (varying along the radius from the optical axis) shift of subjective second-exposure speckles with respect to identical first-exposure speckles in the specklogram plane. The coefficient of scale transformation μ in Eqs. (16) and (17) is connected with the stage of specklogram reconstruction, and it does not determine the speckle interferometer sensitivity to the scatterer longitudinal displacement. It can be seen from the following. From the above conditions:

$$\Delta l \ll R' \text{ и } kL_0^2\mu^2\Delta l\left(x_5^2 + y_5^2\right)/l_1^2l_2^2 << k\mu^2\left(x_5^2 + y_5^2\right)/2\tilde{l},$$

we obtain $\tilde{l} = l_1^2 l_2^2/2L_0^2R'$. Then the optimal value is $l_3 = \tilde{l}$, because for $l_3 < \tilde{l}$ the distribution of the field complex amplitude in the plane of recording a speckle interferogram becomes closer to the distribution corresponding to the field distribution in the far diffraction zone, in which the coincidence of identical speckles of two exposures is absent as a necessary condition for formation of an interference pattern in diffusely scattered fields. In its turn, for $l_3 < \tilde{l}$ the distribution of the field complex amplitude in the plane of recording of a speckle interferogram becomes closer to the distribution corresponding to the field distribution in the plane of the specklogram image formation, in which identical speckles of two exposures do not coincide as well. Consequently, at $l_3 = \tilde{l}$ the speckle interference pattern is maximally contrast, and the use of positive lenses L_0 (see Fig. 4) with different focal lengths f_0 at the stage of specklogram reconstruction leads to different values of the coefficient μ. However, the product of the coefficient μ and the difference between square radii of fringes in neighboring interference orders remains constant.

Assume that, at the reconstruction stage of a double-exposure specklogram characterizing the longitudinal displacement of a diffusely scattering plane surface, the surface displaces in the plane (x_3, y_3) (see Fig. 4), for example, in the direction of the axis x by x_{03}. Then the complex transmission amplitude of the specklogram is determined by the equation

$$\tau'(x_3,y_3) \sim \left\{F(x_3 + x_{03}, y_3) \otimes \right.$$
$$\otimes \exp\left\{-\frac{ikR'L_0^2}{4l_1^2l_2^2}\left[(x_3 + x_{03})^2 + y_3^2\right]\right\} \otimes P(x_3,y_3)\Big\}\{c.c.\} +$$
$$+\left\{F'(x_3 + x_{03}, y_3) \otimes \exp\left\{-\frac{ikR'L_0^2}{4l_1^2l_2^2}\left[(x_3 + x_{03})^2 + y_3^2\right]\right\} \otimes \right.$$
$$\left.\otimes P(x_3,y_3)\right\}\{c.c.\}. \qquad (18)$$

In this case, following the above analysis of formation of the speckle interference pattern characterizing the longitudinal displacement of a scatterer, we obtain the distribution of the complex amplitude of the field in the plane (x_5, y_5) in the form

$$u'(x_5,y_5) \sim \exp\left[\frac{ik}{2l_4}\left(x_5^2+y_5^2\right)\right]\left\{\exp\left[-\frac{ik\mu l_3}{2\tilde{l}l_4}\left(x_5^2+y_5^2\right)\right]\times\right.$$
$$\times\exp\left[\frac{ik\mu^2}{2\tilde{l}}\left(x_5^2+y_5^2\right)\right]\left\{\exp\left[-\frac{ik\mu^2}{2\tilde{l}}\left(x_5^2+y_5^2\right)\right]\otimes\right.$$
$$\otimes\left\{\left\{F_1\left(x_5-\frac{x_{03}}{\mu},y_5\right)\otimes\exp\left\{-\frac{ikR'L_0^2\mu^2}{4l_1^2l_2^2}\left[\left(x_5-\frac{x_{03}}{\mu}\right)^2+y_5^2\right]\right\}\otimes\right.\right.$$
$$\left.\left.\otimes P'(x_5,y_5)\right\}\left\{F_2\left(x_5-\frac{x_{03}}{\mu},y_5\right)\otimes\right.\right.$$
$$\left.\left.\otimes\exp\left\{\frac{ikR'L_0^2\mu^2}{4l_1^2l_2^2}\left[\left(x_5-\frac{x_{03}}{\mu}\right)^2+y_5^2\right]\right\}\otimes P'(x_5,y_5)\right\}+\right.$$
$$+\left\{\exp\left\{\frac{ikL_0^2\mu^2\Delta l}{2l_1^2l_2^2}\left[\left(x_5-\frac{x_{03}}{\mu}\right)^2+y_5^2\right]\right\}F_1\left(x_5-\frac{x_{03}}{\mu},y_5\right)\otimes\right.$$
$$\left.\otimes\exp\left\{-\frac{ikR'L_0^2\mu^2}{4l_1^2l_2^2}\left[\left(x_5-\frac{x_{03}}{\mu}\right)^2+y_5^2\right]\right\}\otimes P'(x_5,y_5)\right\}\times$$
$$\times\left\{\exp\left\{\frac{ikL_0^2\mu^2\Delta l}{2l_1^2l_2^2}\left[\left(x_5-\frac{x_{03}}{\mu}\right)^2+y_5^2\right]\right\}\times\right.$$
$$\left.\times F_2\left(x_5-\frac{x_{03}}{\mu},y_5\right)\otimes\exp\left\{\frac{ikR'L_0^2\mu^2}{4l_1^2l_2^2}\left[\left(x_5-\frac{x_{03}}{\mu}\right)^2+y_5^2\right]\right\}\otimes\right.$$
$$\left.\left.\left.\left.\otimes P'(x_5,y_5)\right\}\right\}\right\}\otimes P_0'(x_5,y_5)\right\}. \qquad (19)$$

Based on this distribution and taking into account the integral representation of the convolution operation with $\exp[-ik\mu^2(x_5^2+y_5^2)/2\tilde{l}]$, the illumination distribution in this plane takes the form

$$I'(x_5,y_5)\sim\left\{1+\cos\left\{\frac{kL_0^2\mu^2\Delta l}{l_1^2l_2^2}\left[\left(x_5-\frac{x_{03}}{\mu}\right)^2+y_5^2\right]\right\}\right\}\times$$

$$\times\left|\exp\left[-\frac{ik\mu l_3}{2\tilde{l}l_4}\left(x_5^2+y_5^2\right)\right]\right\}\left\{\exp\left[\frac{ik\mu^2}{2\tilde{l}}\left(x_5^2+y_5^2\right)\right]\otimes\right.$$

$$\otimes p\left(\frac{l_2\mu}{\tilde{l}}x_5,\frac{l_2\mu}{\tilde{l}}y_5\right)t\left(-\frac{l_1l_2}{\tilde{l}L_0}\mu x_5,-\frac{l_1l_2}{\tilde{l}L_0}\mu y_5\right)\times$$

$$\times\exp\left[\frac{ikl_1^2l_2^2\mu^2}{\tilde{l}^2R'L_0^2}\left(x_5^2+y_5^2\right)\right]\exp\left(\frac{i2k\mu}{\tilde{l}}x_{03}x_5\right)\otimes$$

$$\otimes p\left(\frac{l_2\mu}{\tilde{l}}x_5,\frac{l_2\mu}{\tilde{l}}y_5\right)t^*\left(\frac{l_1l_2}{\tilde{l}L_0}\mu x_5,\frac{l_1l_2}{\tilde{l}L_0}\mu y_5\right)\times$$

$$\left.\times\exp\left[-\frac{ikl_1^2l_2^2\mu^2}{\tilde{l}^2R'L_0^2}\left(x_5^2+y_5^2\right)\right]\exp\left(\frac{i2k\mu}{\tilde{l}}x_{03}x_5\right)\right\}\otimes P_0'(x_5,y_5)\Bigg|^2. \quad (20)$$

If at the stage of double-exposure recording of a specklogram the matte screen *1* (see Fig. 1) is illuminated by the coherent radiation with the convergent spherical wave having the curvature radius $R'=l_1^2/(l_1-L_0)$, then the illumination distribution in the plane (x_5, y_5) is similar to Eq. (20), that is,

$$u'(x_5,y_5)\sim\left\{1+\cos\left\{\frac{kL_0^2\mu^2\Delta l}{l_1^2l_2^2}\left[\left(x_5-\frac{x_{03}}{\mu}\right)^2+y_5^2\right]\right\}\right\}\times$$

$$\times\left|\exp\left[-\frac{ik\mu l_3}{2\tilde{l}l_4}\left(x_5^2+y_5^2\right)\right]\right\}\left\{\exp\left[\frac{ik\mu^2}{2\tilde{l}}\left(x_5^2+y_5^2\right)\right]\otimes\right.$$

$$\otimes p\left(\frac{l_2\mu}{\tilde{l}}x_5,\frac{l_2\mu}{\tilde{l}}y_5\right)t\left(-\frac{l_1l_2}{\tilde{l}L_0}\mu x_5,-\frac{l_1l_2}{\tilde{l}L_0}\mu y_5\right)\exp\left(\frac{ik\mu}{\tilde{l}}x_{03}x_5\right)\otimes$$

$$\left.\otimes p\left(\frac{l_2\mu}{\tilde{l}}x_5,\frac{l_2\mu}{\tilde{l}}y_5\right)t^*\left(\frac{l_1l_2}{\tilde{l}L_0}\mu x_5,\frac{l_1l_2}{\tilde{l}L_0}\mu y_5\right)\exp\left(\frac{ik\mu}{\tilde{l}}x_{03}x_5\right)\right\}\otimes$$

$$\otimes P_0'(x_5,y_5)\Bigg|^2. \quad (21)$$

According to Eqs. (20) and (21), at the stage of specklogram reconstruction, if the specklogram shifts in its plane, interference fringes move ("living" speckle interference fringes) in the direction opposite to the direction of the specklogram shift.

The comparison of application of the holographic interferometer[1] and the speckle interferometer under consideration to the control for the longitudinal displacement of a plane surface, diffusely scattering light, indicates the absolutely different mechanisms of formation of interference patterns in these interferometers. In the holographic interferometer, the formation of interference fringes of equal tilt located both in the hologram plane and in the Fourier plane is caused by the varying (along the radius from the optical axis) tilt of subjective second-exposure speckles with respect to first-exposure speckles. In this case, the spatial filtering of the diffraction field excludes the decorrelation of the speckle fields of the both exposures, which is caused by the inhomogeneous shift of subjective second-exposure speckles in the hologram plane. In the speckle interferometer, the interference pattern is formed only due to the inhomogeneous shift of subjective second-exposure speckles with respect to identical first-exposure speckles in the specklogram plane. At the stage of specklogram reconstruction, the spatial filtering of the diffraction field is necessary, on the one hand, because interference fringes are located in the near diffraction zone and, on the other hand, in order to increase the area, within which the background radiation caused by the constant component of specklogram transmission is excluded, in the plane of recording of the speckle interferogram.

In the experiment, double-exposure specklograms were recorded on Mikrat-VRL photographic plates with the use of the He–Ne laser radiation at $\lambda = 0.6328$ μm. The recorded radiation scattered by the matte screen propagated through the negative lens with the focal length $f = 220$ mm and the pupil diameter $d = 11$ mm, located at a distance $l_1 = 160$ mm. The distance from the lens to the photographic plate was $l_2 = 160$ mm. The diameter of the illuminated area of the matte screen was 40 mm. The experimental technique consisted in the comparison of recorded specklograms for the fixed transversal displacement of the scatterer $a = (0.025 \pm 0.002)$ mm. Different curvature radii of the divergent spherical wave of the radiation used to illuminate the matte screen were in a range $150\ \text{mm} \le R \le \infty$ and $200\ \text{mm} \le R \le \infty$ for the convergent spherical wave.

If the longitudinal displacements of the scatterer by $\Delta l = (0.5 \pm 0.002)$, (1 ± 0.002), and (2 ± 0.002) mm were controlled, the curvature radius R' of the divergent or convergent spherical waves was 252.6 mm.

As an example, Figure 5 shows speckle interferograms characterizing the transversal displacement of the scatterer, recorded in the focal plane of the objective with $f_0 = 50$ mm and the pupil diameter of 17 mm.

At the stage of reconstruction (Fig. 5), the double-exposure specklogram was illuminated by a

collimated beam of 50 mm in diameter. In all cases, as well as in the next, connected with the change of the value and sign of the curvature radius, the periods of interference fringes were measured (in addition, they can be determined from R measurements at known λ, a, f, l_1, l_2, and f_0).

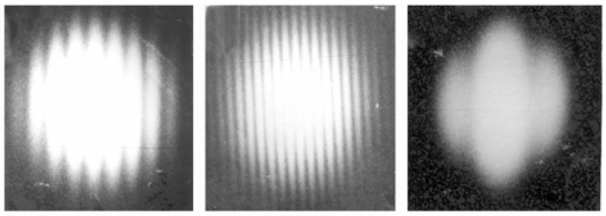

a *b* *c*

Fig. 5. Speckle interference patterns characterizing the transversal displacement of the scatterer and located in the Fourier plane. At the stage of specklogram recording the matte screen was illuminated by the radiation with (*a*) plane wave, (*b*) divergent spherical wave (R = 260 mm), and (*c*) convergent spherical wave (R = 350 mm).

The frequency of the speckle interference fringes obtained in this way corresponds to Fig. 3 accurate to the experimental error (10%). At the stage of reconstruction of double-exposure specklograms characterizing the transversal displacement of the diffusely scattering plane surface, there is no parallax of the interference fringes frozen in the Fourier plane, whose visibility is close to unity due to small value of af_0L_0/l_1l_2 as compared to the negative lens pupil radius.

The speckle interference patterns shown in Fig. 6 are formed upon the reconstruction of the double-exposure specklograms, characterizing the longitudinal displacement of the scatterer, by the collimated beam in the near diffraction zone, when the spatial filtering of the diffraction field are carried out with the aid of the aperture diaphragm p_0 (see Fig. 4) of 2 mm in diameter.

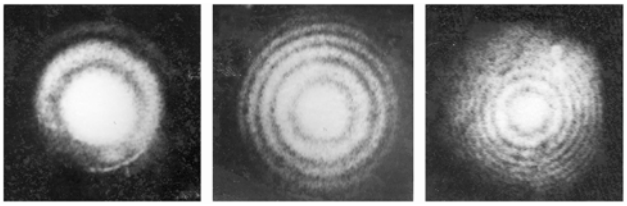

a *b* *c*

Fig. 6. Speckle interference patterns located in the near diffraction zone and characterizing the longitudinal displacement of the diffusely scattering plane surface by Δl = 0.5 (*a*), 1 (*b*), and 2 mm (*c*).

Figure 6*a* corresponds to the case that the matte screen at the stage of specklogram recording is illuminated by the coherent radiation with the divergent spherical wave with the curvature radius R' indicated above, while Figures 6*b* and *c* correspond to the illumination by the convergent spherical wave with the curvature radius R'. In addition, at the stage of specklogram reconstruction, the speckle interferograms shown in Fig. 6 were recorded with the objective having f_0 = 50 mm, whose object plane was at a distance of 754 mm ($\tilde{l} + l_3$), while the distance l_3 was equal to 377 mm. The measurements of the fringe radii in neighboring interference orders correspond to the scatterer displacements Δl = 0.5 mm (see Fig. 6*a*), 1 mm (see Fig. 6*b*), and 2 mm (see Fig. 6*c*) calculated as $\Delta l = 2\lambda l_1^2 l_2^2 / L_0^2 \mu^2 (r_2^2 - r_1^2)$, where r_1 and r_2 are the fringe radii in neighboring orders of interference. This equation follows from Eqs. (16) and (17). The calculations were performed for the scale transformation coefficient μ = 14.1 accurate to the experimental error (10%).

The speckle interference pattern in Fig. 7*a* characterizes the scatterer longitudinal displacement by Δl = 1 mm. This pattern was recorded, like in Fig. 6*b*, in the plane of its localization.

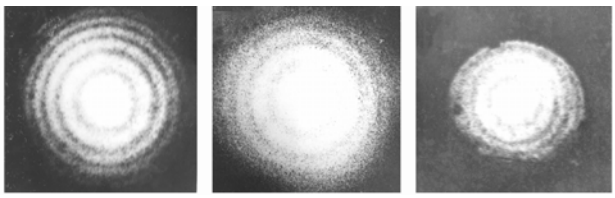

a *b* *c*

Fig. 7. Illumination distributions recorded (*a*) in the plane of localization of the interference patter characterizing the longitudinal displacement of a diffusely scattering plane surface and (*b*, *c*) outside this plane.

At l_3 = 150 mm (Fig. 7*b*), the distribution of the field complex amplitude in the recording plane *3* (see Fig. 4) is closer to the distribution characteristic for the distribution in the far diffraction zone, where identical subjective speckles of both exposures do not coincide. At l_3 = 600 mm (Fig. 7*c*), the distribution of the field complex amplitude in the recording plane is closer to the distribution characteristic of the distribution in the plane of formation of the specklogram image. In both cases, we see the complex character of the correlation degree of subjective speckle fields of two exposures, whose real part determines the visibility of the interference pattern lower than unity and the imaginary part leads to the illumination distribution in the recording plane other than the illumination distribution observed if the speckle interference pattern is recorded in the plane of its localization.

Figure 8*a* (Figure 8*b* is presented for comparison) shows the speckle interferogram, characterizing the longitudinal displacement of the scatterer by Δl = 1 mm.

It was recorded with the objective having the focal length $f_0 = 135$ mm. The object plane at the recording of the speckle interferogram was at a distance of 754 mm $(\tilde{l} + l_3)$, while l_3 was equal to 377 mm.

In contrast to Fig. 8*b*, the diameter of the aperture diaphragm filtering the diffraction field is 4 mm. In addition, the objective angle of view restricts the spatial length of the diffraction halo and, consequently, the speckle interference pattern. The measurements of the fringe radii in neighboring interference orders and the following calculation for $\mu = 4.58$ used in the experiment correspond to $\Delta l = 1$ mm. Both for $f_0 = 50$ and 135 mm, the product of the square coefficient μ by the difference of the square fringe radii in neighboring interference orders is the same.

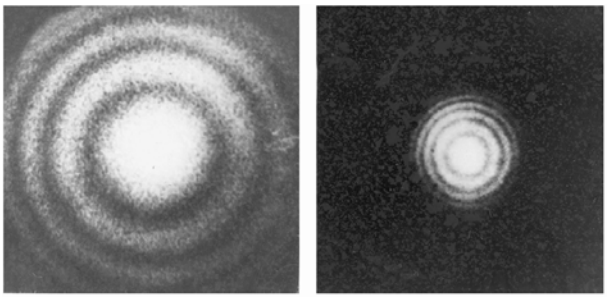

а *б*

Fig. 8. Speckle interference patterns characterizing the longitudinal displacement of the diffusely scattering plane surface and recorded in its plane with the objective having the focal length $f_0 = 135$ (*a*) and 50 mm (*b*).

Figure 9 demonstrates the parallax of interference fringes. For this purpose, the speckle interference pattern was recorded in the plane of its localization with the objective with $f_0 = 135$ mm (Fig. 9*a*). Then the specklogram was displaced in its plane by the distance, at which the interference pattern phase on the optical axis changed by π (Fig. 9*b*).

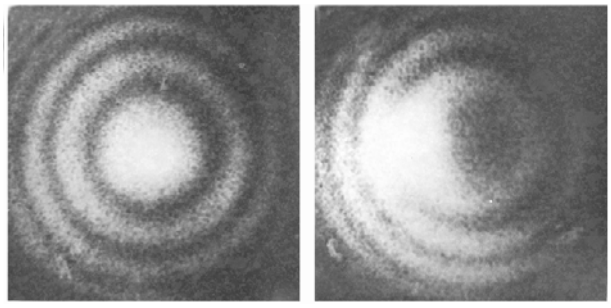

a *b*

Fig. 9. Speckle interference patterns demonstrating the phenomenon of parallax of interference fringes at unshifted (*a*) and shifted (*b*) positions of the specklogram at the stage of its reconstruction.

The measured displacement of the specklogram, equal to 7.7 mm, corresponds to the value following from Eq. (21).

Thus, the results of theoretical analysis and experimental investigations have shown that, at the double-exposure recording of a specklogram with the use of a negative lens, the speckle interferometer sensitivity to the transversal displacement of a diffusely scattering plane surface is the same as the sensitivity of the holographic interferometer, which records the interference pattern located in the Fourier plane. This is explained by the same mechanism of formation of interference patterns, connected with the homogeneous displacement of subjective second-exposure speckles relative to identical first-exposure speckles in the hologram or specklogram plane.

The difference is that frozen interference fringes with the visibility lower than unity are formed regardless of the curvature radius of the spherical wave of coherent radiation used to illuminate the scatterer at the stage of specklogram recording.

In the case that the longitudinal displacement of the diffusely scattering plane surface is controlled, when the scatterer at the stage of double-exposure recording is illuminated by the coherent radiation with the spherical wave having a certain curvature radius, the mechanism of formation of the high-contrast speckle interference pattern in the speckle interferometer, in contrast to the holographic interferometer, is caused by only the inhomogeneous displacement of subjective second-exposure speckles relative to identical first-exposure speckles in the specklogram plane. The sensitivity of the speckle interferometer in this case depends only on the coefficient determining the scale of the Fourier transform of the complex transmission (or reflection) amplitude of the scatterer in the specklogram plane.

The inhomogeneous displacements of subjective second-exposure speckles relative to identical first-exposure speckles in the specklogram plane lead, in their turn, to localization of the speckle interference pattern in the near diffraction zone. The position of the localization plane of the speckle interference pattern in the near diffraction zone depends both on the coefficient determining the scale of the Fourier transform of the complex transmission (or reflection) amplitude of the scatterer in the specklogram plane and on the curvature radius of the spherical wave of coherent radiation used to illuminate the diffusely scattering plane surface.

In addition, the localization of the speckle interference pattern characterizing the longitudinal displacement of the scatterer in the near diffraction zone is accompanied by the phenomenon of parallax, that is, by the observation of "living" interference fringes.

References

1. V.G. Gusev, Atmos. Oceanic Opt. **19**, No. 5, 407–416 (2006).
2. J.W. Goodman, *Introduction to Fourier Optics* (Mc.Graw-Hill, New York, 1968).
3. V.G. Gusev, Opt. i Spektrosk. **69**, No. 5, 1125–1128 (1990).
4. Motoki Yonemura, Optik. **63**, No. 2, 167–177 (1983).
5. C. M. Vest, *Holographic Interferometry* (Wiley, New York, 1979).
6. V.G. Gusev, Opt. i Spektrosk. **74**, No. 6, 1201–1206 (1993).
7. M. Franson, *Laser Speckle and Applications in Optics* (Academic, New York, 1979).
8. V.G. Gusev, Elektron. Tekhn. Ser. 11. Lazer. Tekhn. i Optoelektron., No. 3, 51–55 (1991).
9. V.G. Gusev, Opt. Zh., No. 1, 9–12 (1993).
10. R. Jones and C. Wykes, *Holographic and Speckle Interferometry* (Cambridge U. Press, Cambridge, UK, 1983).